MCs$^+$ Molecular Ion Formation Under Varying Alkali Metal Environment

Biswajit Saha

Assistant Professor
Department of Physics
Uluberia College, Uluberia
Howrah, West Bengal, India -711315

Email: biswajit.saha09@gmail.com

Abstract— The objective of the present paper is to investigate the mechanism of MCs$^+$ molecular ion production with variable Cs impact energy by examining the emission of various atomic and molecular ions from the surface of elemental molybdenum when bombarded with Cs$^+$ under secondary ion mass spectrometry (SIMS) study. Increasing primary ion energy is accompanied by a monotonic rise in MoCs$^+$ molecular ion intensity. The observation is explained by the difference in the surface work function (ϕ) and fractional surface concentration (c$_{Cs}$) brought on by different impact energy. It appears that ϕ is linearly dependent on c$_{Cs}$. To explain the MoCs$^+$ data, a phenomenological model has been used, which is based on ϕ's linear dependency on c$_{Cs}$.

I. INTRODUCTION

Ion beam induced sputtering is a well-developed and established technology for analyzing surfaces, interfaces, and bulk materials. The 'sputtering-yield', which is defined as the mean number of emitted atoms per incident ion, is used to estimate the ejection of surface atoms or molecules under energetic ion impact (in the range of few hundred eV to several MeV). In this process, the bombarding ion transfers energy in collisions to target atoms, which recoil with enough energy to generate other collisions. Some of the backward recoils in the created 'collision cascade' give the surface atoms enough energy to overcome the surface binding energy and escape from the solid. Therefore, the collision cascades within the target lattice and recoil sputtering are the sources of the secondary sputtered species.

The sputtering yield in the linear cascade regime depends on the quantity of recoil-atoms, which depends on the amount of energy deposited per unit depth in nuclear processes (particle velocity significantly lower than the Bohr velocity). The effective layer thickness following a single collision cascade is on the order of an atomic dimension, and its estimation can be obtained from a straightforward expression of the sputtering-yield involving information depth, typical average particle energy, and nuclear stopping power [1]. The expelled particles, which generally come from the outermost (~1-3) atomic layers, include stoichiometric information about the area close to the surface. Sputter-products come in a variety of forms, including electrons, atoms, atomic clusters, molecules 'intact', and unique molecular fragments. A very small percentage of the sputtered atoms or molecules may be excited above their respective ground states and/or ionized, either positively or negatively.

Eur. Chem. Bull. **2022**,*11 (Issue 4), 185 – 191*

185

Following their sputtering in the excited states, the atoms (or ions) may undergo one of two inelastic processes:

A. Radiative electronic transition involving the excited neutral (or ionic) species' de-excitation, which results in the emission of photons with wavelengths ranging from ultraviolet to visible region.

B. A non-radiative electronic transition that causes the sputtered species to ionize or emit Auger electrons by resonantly tunnelling electrons from these species to the solid's valence band.

The high electronic and structural perturbations brought on by the ion bombardment further complicate the dynamic charge-transfer processes described above that take place between the fleeing sputtered atom and the solid surface.
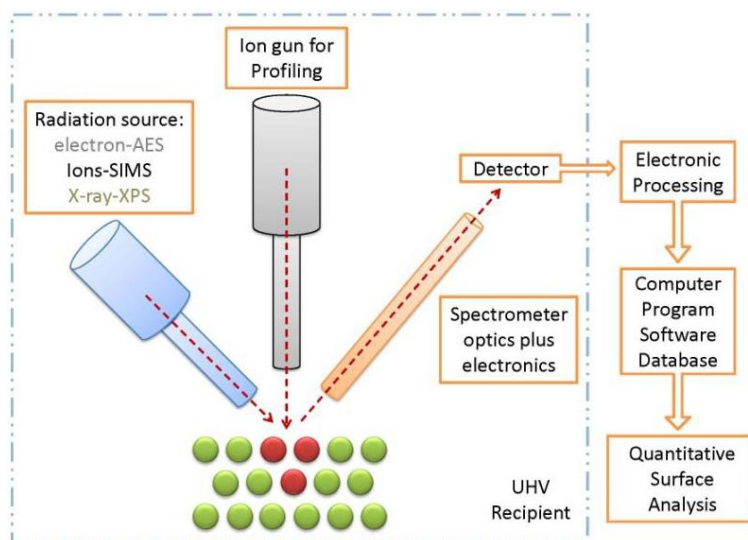
II.   SECONDAY IONS AND MATRIX EFFECT

Fig.1. Schematic showing instrumental parts and principal arrangement of a surface analysis instrument for sputter depth-profile analysis.

The sputtering process causes secondary emission of ions and photons, which is an inelastic phenomena in ion-surface interactions and has crucial applications in materials investigation. The 'Secondary Ion Mass Spectrometry' (SIMS), which detects the ionised fraction of the sputtered species (also known as secondary ions) by a mass spectrometer outfitted with suitable ion collection optics, is one of the important analytical sputtering techniques based on the aforementioned phenomenon. The technique's schematic representations are shown in Figure 1. In this method, the intensity, mass, and energy of the bombarding ions as well as the physical and chemical properties of the sample itself dictate how quickly the primary beam removes the sample's atomic (or molecular) layers. Despite SIMS having the highest detection sensitivity (down to the part-per-billion level) and best depth resolution (down to less than 2 nm), the 'matrix effect' (variation in the ionisation probability of a specific species due to an instantaneous change in the local surface chemistry of the target containing the species) makes it difficult to quantify samples. Through SIMS analyses of Pt/Cu and Au/Cu multilayers, it was shown that the typical matrix effect occurs when oxygen is preferentially trapped in these multilayer structures, as seen by the huge humps for Pt and Au signals across the interface sites in the corresponding multilayers [2]. It goes without saying that the matrix effect needs to be properly corrected when determining the precise concentration of a particular species present in the host (or

Eur. Chem. Bull. **2022**,*11 (Issue 4), 185 – 191*

186

'matrix'). In order to compensate, 'calibration standards', 'relative sensitivity factor' (RSF) method, etc. are typically used [1]. Precision measurements are now possible in SIMS quantification thanks to the high level of complexity obtained by the use of 'ion-implanted standards'. The invention of a different method known as 'secondary neutral mass spectrometry' (SNMS), from an analytical standpoint, was motivated by the need to reduce the matrix effect. However, despite the complexity of the ionisation mechanism, most workers focus on the secondary ion emission process for analytical work because sputtering neutral signals are fundamentally much less intense than the secondary ion signals. Although very comprehensive theoretical treatments of the ionisation process have been produced for idealised models [3-8], a quantitative theory that takes into consideration the dynamic evolution of the sputtering collision cascade and the chemical complexity of real materials is still lacking.

III.   MCs⁺ ION EMISSION: POSSIBLE MECHANISMS

The MCs⁺ methodology appears to be the most effective and promising approach for reducing the matrix effect in SIMS analysis. Since it has been demonstrated that the detection of the target element M under Cs⁺-bombardment can be quantified without the use of calibration standards by monitoring MCs⁺ molecular ions (instead of traditional M ions) [5, 6], this mode of analysis is largely unaffected by matrix changes. The MCs⁺ detection system is more advantageous in situations when matrix effects are most severe, particularly for significant components, despite the fact that its weak sensitivity makes application problematic (MCs⁺ molecular species are typically less common than the atomic ions). Thus Cs⁺-assisted secondary ion mass spectrometry, also known as MCs⁺-SIMS, is a cutting-edge method that has been successfully applied for several measurements.

Several researchers have looked at the mechanism behind the formation of MCs⁺ secondary ions as well as the analytical applicability of the MCs⁺-SIMS technique [10, 11]. Based on several experimental findings, it was postulated that independently sputtered neutral M^0 atoms and Cs⁺ ions recombine together to produce MCs⁺ molecular ions. Since the interaction is primarily between the electric field of Cs⁺ ion and the ion-induced dipole moment of M, it is clear that the binding energy between M and Cs (either charged or neutral) plays a crucial role in the formation of the MCs molecule. In this case, the polarizability of M also plays a key role in the binding strength of the two species. A potential $V(r)$ of the following form has successfully been used to simulate the interaction between Cs⁺ and a polarizable neutral atom (or molecule).

$$V(r) = Ar^{-12} - \frac{1}{2}\alpha e^2 r^{-4}$$

where r is the separation between the neutral atom and the Cs⁺ ion, α is the former's polarizability, and A is a constant that describes the repulsive term. The polarizability of the atom M was found to have a quadratic dependence on the MCs⁺ yield for a number of semiconductors [12]. Although, several works have reported the mechanism of MCs⁺ molecular ion formation [8–10], the dependence of MCs⁺ formation on primary the cesium ion impact energy has not been systematically investigated so far. The present paper reports a comprehensive study of secondary MCs⁺ emission from molybdenum surfaces under varying Cs impact energy.

IV.   EXPERIMENTAL DETAIL

The experiment was conducted using spectroscopically pure (99.95%, Alfa Aesar) polycrystalline molybdenum foil. Molybdenum was chosen because of its comparatively high atomic polarizability, which is crucial for the formation of the molecular ion MCs⁺. Prior to the actual data acquisition, the sample was extensively cleaned with trichloroethylene in an ultrasonic bath and then sputter cleaned to

Eur. Chem. Bull. **2022**,*11 (Issue 4), 185 – 191*

187

remove the native oxide layer from the surface. A quadrupole mass spectroscopy-based SIMS apparatus (HIDEN Analytical Ltd., UK) was used for the SIMS research. According to calculations made using the energy analyser's geometry, its energy resolution typically ranged from 0.003 to 0.679 eV for a transmission energy range of 0.05 to 25.0 eV. The base pressure was 6.8×10^{-9} mbar. Primary ion current (25–60 nA) was maintained while the target was bombarded with 1-5 keV Cs^+ primary ions at an impact angle of 22.5 with the surface normal. By scanning the voltage of the electrostatic energy analyzer in 0.05 V increments, the energy distributions of Cs^+, Cs_2^+, and $MoCs^+$ were recorded for various primary ion impact energies.

V. RESULTS AND DISCUSSION

As the impact energy (E) of the primary cesium beam increases, the integrated count of re-sputtered Cs^+ also increases monotonically (Fig. 2a). The intensity of the re-sputtered Cs^+ ion is determined by

$$I_{Cs} \propto Y c_{Cs} \beta^+ \tag{1}$$

where Y is the overall sputtering yield, c_{Cs} represents the fractional surface concentration of Cs, and β^+ represents the ionization probability of Cs. Now, there is a significant correlation between the primary ion impact energy E and the total sputtering yield Y and Cs surface concentration c_{Cs}. Y has been calculated for various impact energies using the TRIM code. Figure 2b depicts the relationship between Y and E. Ionisation probability β^+ is dependent on the surface work function ϕ and ionisation potential I of the sputtered atom, per the electron tunnelling model [3] and is given by

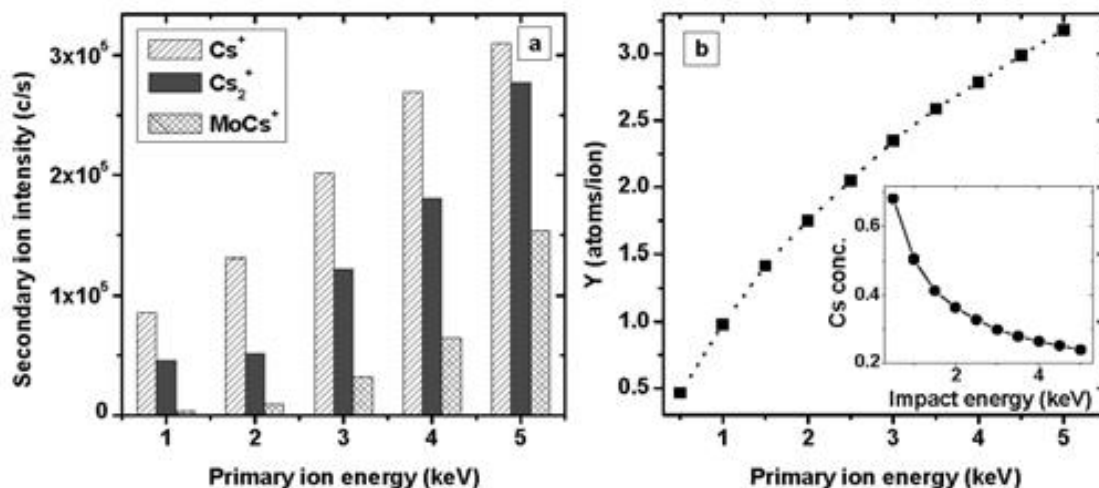$$\beta^+ \propto exp[-(I-\phi)/\epsilon_0] \tag{2}$$

Fig.2: (a) Intensity of secondary ions as a function of E and (b) Y as a function of E; Inset: c_{Cs} vs. E.

The normal component of the secondary ions' emission velocity is thought to be what determines the parameter ϵ_0 [13]. The bombardment parameters in dynamic SIMS define the value of c_{Cs}. Several studies [14] have shown that the maximum cesium surface concentration that can be achieved during cesium bombardment is directly related to the sputtering yield of cesium in the material according to $c_{Cs} \propto 1/(1+Y)$. This formula is predicated on the notion that, in a stationary environment, the flux of incident and sputtered cesium is equal. Figure 2b inset shows how c_{Cs} changes as impact energy increases. It

Eur. Chem. Bull. **2022**,*11 (Issue 4), 185 – 191*

188

implies that the steady state fractional surface concentration of cesium is lower the higher the impact energy of cesium. In the present study, the range of c_{Cs} is 0.24 to 0.50. However, this variation in cesium surface concentration has the potential to significantly alter the surface work function [14]. The energy distributions of Cs⁺ for various cesium impact energies are shown in Figure 3a. With rising cesium impact energy, a clear shift in the spectra is seen. The surface work function declines linearly ($\Delta\phi_{max}$= 0.69 eV) with increasing cesium concentration, according to a measure of the relative changes in the surface work function obtained from the leading edges of the Cs⁺ energy distributions (Fig. 3b). Given that has a linear relationship with c_{Cs}, one can write

$$\phi = \phi_0 - kc_{Cs} \tag{3}$$

where ϕ_0 is the initial work function and k is a constant. Using Eqs. (2) and (3), Eq. (1) can be written as
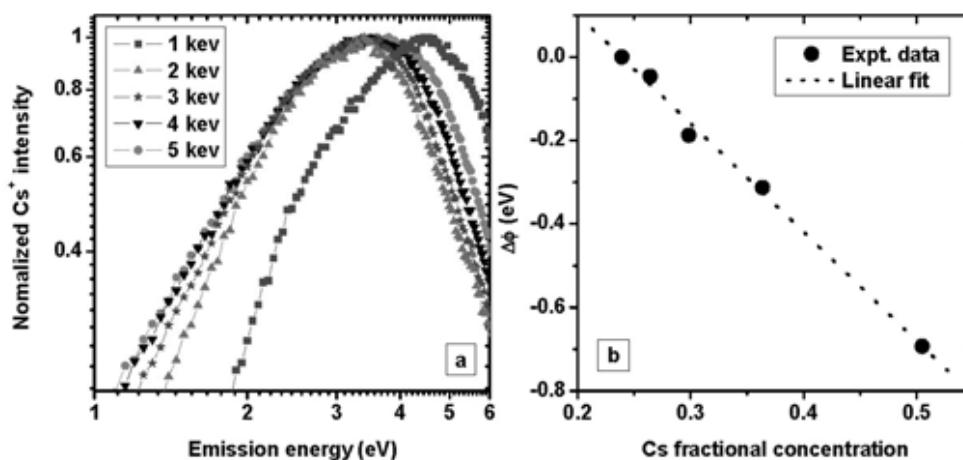
$$I_{Cs} = CY_{Cs}\exp(-kc_{Cs}) \tag{4}$$

Fig.3: (a) Cs⁺ energy distribution as a function of impact energy and (b) $\Delta\phi$ as a function of c_{Cs}.

Here, *C* and *k* are constants. Since the studies were conducted with steady-state Cs⁺ bombardment, the surface stoichiometry must be adjusted to provide a partial Cs sputter yield of unity. Thus, unity is used to replace the product Yc_{Cs}. Figure 4a depicts the change in Cs⁺ intensity as a function of cesium surface concentration. For k_{Cs}= 5.93±0.79, the best fit is discovered. If the recombination mechanism is taken into account for the generation of Cs₂⁺, the relation [14], can be used to express Cs₂⁺ intensity.

$$I_{Cs_2} = C\{1 - A\exp(-kc_{Cs})\}\exp(-kc_{Cs}) \tag{5}$$

Here, it is assumed that f_{Cs2}, the probability of Cs₂⁺ production, is constant. With $k_{Cs2} = 6.62±1.32$, the Cs₂⁺ data are best fit (Fig. 4a). This value of *k* exhibits good agreement with the Cs⁺ value. This finding suggests that the recombination of neutral Cs⁰ atom with Cs⁺ ion appears to be the most likely to produce Cs₂⁺ molecule ion in the current condition. As the bombarding energy of the Cs⁺ primary ion increases, so does the intensity of MoCs⁺ (Fig. 2a). The formula for MoCs⁺ ion intensity is

$$I_{MoCs} \propto Yc_{Mo}\beta^+ Yc_{Cs}f_{MoCs} \tag{6}$$

where c_{Mo} is the concentration of Mo and f_{MoCs} is the formation probability of MoCs⁺ molecular ion. Now using Eqs. (2) and (3) we have

Eur. Chem. Bull. **2022**,11 (Issue 4), 185 – 191

189

$$I_{MoCs} = AY(1 - c_{Cs})\exp\left(-kc_{Cs}\right)f_{MoCs} \tag{7}$$

Here A is a constant. The best fit for the MoCs$^+$ data (Fig. 4b) is obtained for k_{MoCs} = 6.34 $\pm$ 0.76. The value of k obtained for MoCs$^+$ is quite close to what we have obtained for Cs$^+$ data. This observation strengthens the belief that the MoCs$^+$ molecular ions form via the combination of neutral Mo atoms with the Cs$^+$ ions.
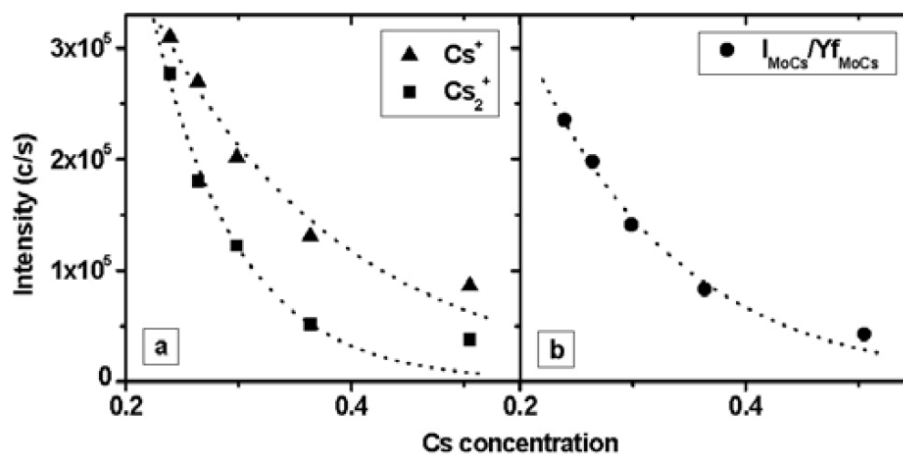

Fig.4: Intensity of (a) Cs$^+$, Cs$_2^+$ and (b) MoCs$^+$ as a function of cesium.

VII. CONCLUSION

Secondary emission of atomic and molecular ions from elemental molybdenum surface has been studied under Cs$^+$ bombardment to explore the MCs$^+$ formation mechanism with changing Cs surface coverage. Change in MoCs$^+$ intensity is attributed to the variation of surface work function ϕ and cesium surface concentration c_{Cs} due to varying impact energies. Surface work function is found to decrease with increasing cesium concentration, which in turn decreases, with increasing cesium impact energy. Surface work function shows a linear dependence on the cesium concentration. Emission of all atomic and molecular ionic species has been found to be consistent with the electron-tunneling model.

REFERENCES

1. P. Chakraborty, Ion Beam Analysis of Surfaces and Interfaces of Condensed Matter Systems ed. P. Chakraborty, New York, Nova Science, 2002.
2. S. Sarkar and P. Chakraborty, "Preferential Oxygen-Trapping in Metallic Multilayers: A SIMS Perspective", J. Chinese Chem. Soc. 48, Sep. 2000, pp. 521-524.
3. P. van der Heide, Secondary Ion Mass Spectrometry: An Introduction to Principles and Practices, John Wiley & Sons Inc, 2014
4. K. Schaepe, H. Jungnickel, T. Heinrich, J. Tentschert, A. Luch, and W. E. S. Unger, Secondary ion mass spectrometry, Characterization of Nanoparticles, 2020, pp. 481–509.
5. M. Haag, H. Gnaser and H. Oechsner, "MCs$^+$ secondary ion and sputtering yields of oxygen-exposed semiconductors and glasses", Fresenius' J. Anal. Chem. 353, 1995. pp. 565-569.
6. Y. Gao, "A new secondary ion mass spectrometry technique for III-V semiconductor compounds using the molecular ions CsM$^+$", J. Appl. Phys. 64, 1988, pp.3760-3762.

Eur. Chem. Bull. **2022**,*11 (Issue 4), 185 – 191*

190

7. C. W. Magee, W. L. Harrington and E. M. Botnick, "On the use of CsX$^+$ cluster ions for major element depth profiling in secondary ion mass spectrometry", Int. J. Mass Spectrom. Ion Proc., 103, 1990, pp. 45-56

8. K. Wittmaack, "Angular dependence of ion yields and cesium surface coverage in Cs$^+$ attachment secondary ion mass spectrometry (CsAMS)", Nucl. Instrum. Meth. in Phys. Res. B 85, Mar. 1990, pp. 374-378.

9. J. Brison, R. Hubert, S. Lucas and L. Houssiau, "Study of the Pd–Rh interdiffusion by ToF-SIMS, RBS and PIXE: Semi-quantitative depth profiles with MCs$^+$ clusters", Appl. Surf. Sc. 252, Jul. 2006, pp. 7038-7040.

10. J. Schroer, H. Gnaser and H. Oechsner, SIMS IX eds. A. Benninghoven et al, New York, Wiley, 1993.

11. U. Breuer, H. Holzbrecher, M. Gastel, J.S. Becker and H.H. Dietz, "Comparative studies of MCs$^+$-SIMS and e$^-$-beam SNMS for quantitative analysis of bulk materials and layered structures", Fresenius' J. Anal. Chem. 353, Jan 1995, 372-377.

12. H. Gnaser and H. Oechsner, "The influence of polarizability on the emission of sputtered molecular ions", Surf. Sci. Lett. 302, Jan. 1994, pp. L289-L292.

13. M. L.Yu and N.D.Lang, "Direct Evidence of Electron Tunneling in the Ionization of Sputtered Atoms", Phys. Rev. Lett. 50, January 1983, pp.127-130.

14. B. Saha, S. Sarkar, P. Chakraborty and H. Gnaser, "Secondary emission of MCs$_n^+$ molecular ions under the joint influence of electropositive and electronegative elements", Surf. Sci. 602, Mar. 2008, 1061-1065.

Eur. Chem. Bull. 2022,11 (Issue 4), 185 – 191

191